Astron. Astrophys. 201, 299–310 (1988)

ASTRONOMY
AND
ASTROPHYSICS

Observational evidence for the influence of the magnetic field on star formation in the Serpens molecular cloud

A.I. Gomez de Castro [1], C. Eiroa [1,⋆,⋆⋆], and R. Lenzen [2]

[1] Observatorio Astronomico Nacional, c) Alfonso XII, 3, E-28014 Madrid, Spain
[2] Max-Planck-Institut für Astronomie, Königstuhl, D-6900 Heidelberg 1, Federal Republic of Germany

Received December 16, 1987; accepted March 10, 1988

Summary. We present new optical and infrared observations of the Serpens star-forming region.

Seven nebulous objects have been detected at 0.9 μm in a region of 20 arcmin^2 in size within the Serpens dense molecular core. Two objects are bipolar nebulae – the Serpens reflection nebula (SRN) and a new very faint nebulosity – and five have a cometary-like shape with a stellar object at the apex. We propose that all the seven objects are reflection nebulae. An analysis of the extinction by means of the Hubble's relation suggests the presence of a dust disk or torus around the illuminating stars. The major symmetry axis of the nebulosities and other young objects within the observed region is correlated with the helical component of the interstellar magnetic field. This is interpreted in terms of the role played by the field in the star-forming processes in the Serpens cloud. A star formation efficiency of around 10% and a stellar mass density of several hundreds $M_\odot$ pc^{-3} are implied from the observational data. These results suggest the formation of a bound stellar cluster.

Two distinct polarization patterns are seen at 0.95 μm in SRN: The typical centro-symmetric orientation of the electric vectors in bipolar nebulae, and a noncentro-symmetric band around the exciting star. This band coincides with the dust disk of the nebula. A 2.2 μm map of SRN shows several point-like sources and extended emission which is the infrared counterpart of the reflection nebulosity.

The new detected bipolar nebula coincides with the near-infrared/radio continuum source SVS4. This is the only object which significantly departs from the common orientation of the Serpens objects. In addition, a 2.2 μm map of SVS4 shows that the infrared emission actually comes from several distinct point-like sources.

Key words: interstellar medium: molecular clouds: Serpens – interstellar medium: magnetic field – interstellar medium: reflection nebulae – stars: pre-main-sequence – stars: clusters

Send offprint requests to: C. Eiroa (Madrid)

⋆ Visiting Astronomer in the Institute for Astronomy, University of Hawaii

⋆⋆ Visiting Astronomer at the United Kingdom Infrared Telescope, which is operated by the Royal Observatory of Edinburgh on behalf of the U.K. Science and Engineering Research Council

1. Introduction

A considerable amount of work has been dedicated to the Serpens region since it was recognized by Strom et al. (1974) as a site of active star formation.

The region attracted the attention of Strom et al. (1974) because of a very red bipolar-shaped nebulosity located several arcminutes west of S68 (Sharples, 1959). An infrared point source placed to the south of this nebula was first proposed as the exciting star. However, polarization measurements showed that the nebula is illuminated by a star seen at the apex of the northwestern lobe (Worden and Grasdalen, 1974; King et al., 1983). This star has been classified as late B or early A, recently arrived at the main sequence, and obscured by 8 mag of visual extinction, although a spectral type M0 and an extinction of 4 mag has also been proposed (Cohen and Kuhi, 1979). Further optical work on the region has been done by Gyulbudaghian et al. (1978, hereafter GGD), Hartigan and Lada (1985, hereafter HL), Chavarria et al. (1987) and Warren-Smith et al. (1987a). GGD found a nebulous object to the north-east of SRN which they catalogued in their list of suspected Herbig-Haro objects as object 29. HL carried out intensive CCD observations of the region. Additional CCD imaging and polarimetry have been done by Warren-Smith et al. (1987a). The work of Chavarria et al. (1987) provided for the first time a reliable estimate of the distance and interstellar extinction to Serpens. A previous estimate by Strom et al. (1974) was based on insufficient observations of the star BD + 1°3694. The distance estimated by Chavarria et al. (1987) is 250 pc. In this paper we will assume this value; therefore, all distance-dependent parameters quoted from other works have been reduced to this distance.

Near-infrared observations of the region carried out by Strom et al. (1976, hereafter SVS) detected 20 infrared sources, several of them with infrared colours consistent with those expected from pre-main-sequence (PMS) stars. Churchwell and Koornneef (1986, hereafter CK) observed further 2.2 μm sources near the Serpens nebula and detected the 3.1 μm ice absorption feature toward 4 of these objects. The most prominent near-infrared sources are SVS2 (CK3), which is the exciting star of SRN, SVS4 and SVS20 (CK1). This latter source is a double PMS star whose components have a mass of 1–2 $M_\odot$, and have not reached the T Tauri stage yet (Eiroa et al., 1987; Eiroa and Leinert, 1987). Based on speckle observations of the 3.1 μm ice feature, Eiroa and Leinert (1987) deduced that the ice-carrying grains are distributed

on a large scale within the Serpens intracloud medium as suggested by the observational results of CK. Far infrared extended emission has been detected by Nordh et al. (1982), Harvey et al. (1984) and IRAS. These observations also revealed that the most luminous object in the region is a far infrared point-like source, FIRS 1, located to the west of SRN, and with a luminosity of around $75\,L_{\odot}$.

Several compact radio continuum sources in the direction of Serpens have been found by Rodriguez et al. (1980) and Snell and Bally (1986). One source is located at the position of the near infrared source SVS4; the other three sources form a group coincident with FIRS 1. In all the cases the luminosity deduced from the radio data exceeds the total infrared luminosity, suggesting that the radio sources are not normal compact H II regions. Two H_2O masers have also been observed at the position of FIRS 1 (Blair et al., 1978; Rodriguez et al., 1978, 1980; Dinger and Dickinson, 1980). CO and OH molecular outflows in the direction of Serpens have been observed by Loren et al. (1981). Bally and Lada (1983), Mirabel (1987), and Clark and Turner (1987). In addition, Nordh et al. (1982) also reported high velocity CO-wings at the position of SVS4.

CO, NH_3, HCO, and H_2CO molecular radio observations have been carried out by several groups (Loren et al., 1979, 1981; Loren and Wooten, 1980; Ho and Barret, 1980; Rodriguez et al., 1980; Little et al., 1980; Ungerechts and Gusten, 1984). All these observations show that the region is a large molecular cloud where low mass star-forming processes are taking place. An H_2CO dense core of radius 0.24 pc and mass $220\,M_{\odot}$ is centered at the position of the red nebula (Loren et al., 1979).

In this paper we present new, more sensitive direct and polarimetric CCD observations of the Serpens region, as well as new infrared photometry of several sources and 2.2 μm maps of the fields around SRN and the infrared source SVS4. We found that the cloud core is densely populated with young objects, most of them in a phase of mass outflow, and that the major axis of the outflows lies approximately parallel to the local magnetic field. In this sense, the Serpens cloud, and in particular its most prominent object, SRN, appears to be suited for comparing the predictions of theoretical models about magnetized molecular clouds with high quality observational data.

2. Observations and results

The observations reported here have been carried out at the Calar Alto Observatory, Spain, using the 3.5 m and the 2.2 m telescopes. In addition, a part of the near-infrared observations were made with the United Kingdom 3.8 m Infrared Telescope on Mauna Kea Observatory, Hawaii.

2.1. CCD direct images at the CA 3.5 m telescope

The 3.5 m CCD images were carried out at the prime focus of the 3.5 m telescope on August 1985 using a 576 × 385 pixel GEC CCD combined with a RG 830 filter (*I* band). This combination provides a field of view on the sky of 166″ × 110″ (0.″288/pixel) and the effective wavelength is $\lambda = 9140$ Å, with $\Delta\lambda = 2000$ Å at the 10% level; thus the transmission range is similar to the Johnson *I*-band. The seeing during these observations was about 1″. Several exposures of different fields of the region were taken. The center of each image and the exposure times are given in Table 1. Flat field correction and dark substraction of each frame have been made using standard procedures. Very short exposures of the star SAO 123565 were carried out inmediately before each Serpens CCD frame. This star has been used as an offset star and also to calibrate photometrically the frames of Table 1. We estimate a magnitude error of about 0.3 mag, this value being mainly due to zero-point uncertainties, statistical noise and variation in counts from the aperture size chosen around the objects. The estimated limiting magnitude is 23 mag for point sources and an exposure time of 1200 seconds. Position errors are 1″. Figure 1 reproduces a mosaic built up from the Serpens-fields. The total area observed at 0.9 μm is about 20 arcmin^2 in size. A relatively high number of reddened stars and stars associated with nebulosity are seen in the region. Table 2 gives the position and *I* magnitude of most of these stars. Our *I* magnitudes are in agreement with the values reported by HL, the small differences are due to the different effective wavelengths and to the contamination produced by nebulosity in some stars. In the table, other designations of the objects are also indicated and are taken from the works of SVS, GGD, HL, and CK.

Table 1. Observed Serpens fields at 0.9 μm with the 3.5 m Calar Alto telescope

Field	α(1950)	δ(1950)	Exposure time (s)
1	$18^h27^m20^s.1$	1°13′18″.0	1200 + 1200
2	$25^s.9$	10′55″.0	900 + 1200 + 1200
3	$26^s.2$	13′02″.0	600
4	$26^s.4$	12′16″.0	900 + 1200
5	$30^s.6$	13′19″.0	900 + 900
6	$31^s.7$	14′37″.0	900

The most outstanding object is the Serpens Reflection Nebula, SRN. It is characterized by a rather complex bipolar structure with several knots of gas and dust embedded in both nebular lobes. The size of SRN on the *I* photographs is about 2.′5 and it is orientated in the southeast-northwest direction. The southeastern lobe is large and diffuse except in the regions close to the exciting star, No. 6 in Table 2 (Worden and Grasdalen, 1974). The northwestern lobe is a little bit smaller, although brighter and more uniform. Several condensations are seen in both lobes whose positions and integrated I magnitudes are given in Table 3.

A second, previously unknown, very faint bipolar nebula, object No. 11 in Table 2, is detected at the position of the infrared/radio source SVS4 (SVS, Rodriguez et al., 1980). In addition, five objects listed in Table 2 are stars associated with a cometary-like nebulosity each. Three of them (Nos. 12, 17, and 18) are visible on the Palomar Sky Survey. Nos. 12 and 17 have also been detected at infrared wavelengths by SVS and CK. No. 18 is number 29 in the list of suspected HH objects of GGD; one star is located 7″ to the southeast of this object, although with the present data we cannot establish if the star is related to No. 18 and the Serpens cloud (see also Warren-Smith et al., 1987a). The other two cometaries Nos. 5 and 15 are new detections; 15 coincides with the 2 μm source CK 6. Object 10 is a PMS double star previously discussed by us (Eiroa et al., 1987; Eiroa and Leinert, 1987). The rest of the objects in Table 2 are reddened stars. Several of them are known 2 μm sources and in most of the cases they probably are field stars. Finally, no object has been detected at the position of FIRS1 and its associated H_2O maser and radio continuum sources (Rodriguez et al., 1980; Harvey et al., 1984).

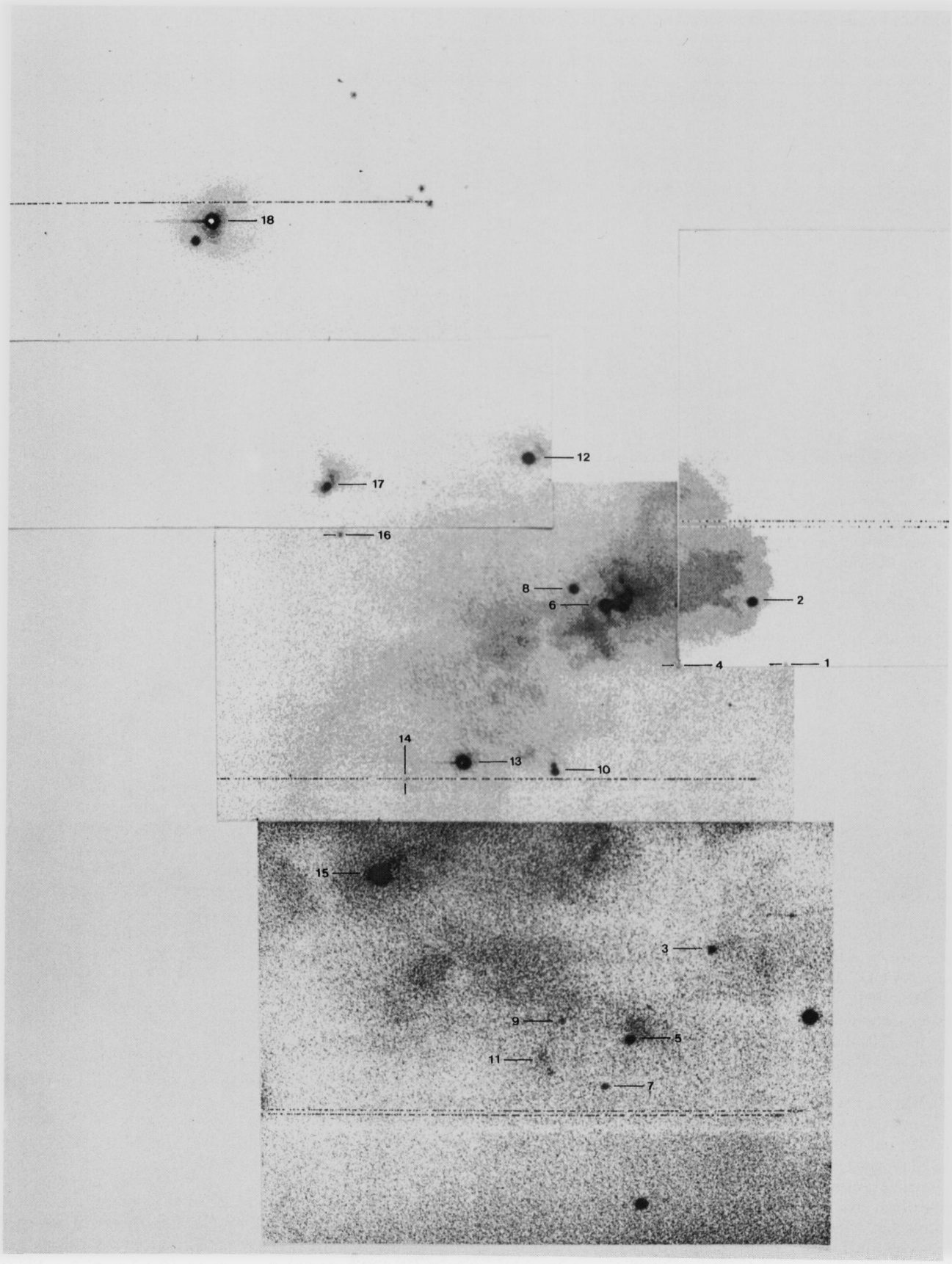

Fig. 1. CCD $I(\lambda = 9140$ Å) image of the Serpens region. The photograph is a mosaic built up from individual CCD images (see Table 1). Each of these has different contrast in order to enhance the most significant features of the field. The position and I magnitude of the numbered objects are given in Table 2. North is at the top and east to the left

Table 2. Position and I magnitudes of some stars in the Serpens field

Number	Other designations	α(1950)	δ(1950)	I	Notes
1		$18^h27^m21^s.49$	1°12′25″.9	19.5	
2		22^s.08	12′41″.6	16.8	
3		22^s.74	11′14″.2	19.8	
4	CK9	23^s.27	12′25″.5	19.8	
5		24^s.15	10′50″.9	18.9	a
6	SVS2, HL2, CK3	24^s.50	12′41″.0	15.0	b
7		24^s.58	10′38″.8	20.4	
8	HL3	25^s.04	12′44″.9	16.4	
9	CK5	25^s.29	10′55″.9	21.8	
10	SVS20, HL16, CK1	25^s.38	11′58″.6	16.9	c
11	SVS4	25^s.44	10′42″.9	21.3	d
12	CK4	25^s.86	13′17″.3	15.7	a
13	CK8	26^s.92	12′00″.9	14.0	
14		27^s.92	11′56″.6	19.6	
15	CK6	28^s.38	11′32″.6	18.0	a
16	CK12	28^s.98	12′58″.7	19.1	
17	SVS1, HL15	29^s.30	13′10″.3	17.3	a
18	GGD29, HL18	31^s.26	14′16″.4	14.5	a

Notes: SVS: Strom et al. (1976); GGD: Gyulbudaghian et al. (1978); HL: Hartigan and Lada (1985); CK: Churchwell and Koornneef (1986)
a: star associated with a cometary nebula; b: exciting star of SRN; c: double PMS star; d: point-like object embedded in a faint bipolar nebula

Table 3. Position and integrated I magnitude of several condensations within SRN

Condensation	α(1950)	δ(1950)	I
C1	$18^h27^m24^s.2$	1°12′41″.0	19.2
C2	24^s.8	34″.1	18.4
C3	25^s.9	36″.3	19.3
C4	26^s.0	31″.6	19.3
C5	26^s.3	28″.3	19.8

2.2. CCD direct images at the CA 2.2 m telescope

The observations at the 2.2 m telescope, were made in June 1984 using a RCA CCD. The scale in this case is 0″.34/pixel and the field of view 174″ × 106″. The seeing was about 1″. At this telescope the frames were only made at a position approximately centered in SRN. A RG 780 filter ($\lambda_{eff} = 8390$ Å, $\Delta\lambda = 1900$ Å at the 10% level) and red filters with effective wavelengths $\lambda = 6640$ Å (FWHM = 280 Å), $\lambda = 6657$ Å (Hα, FWHM = 100 Å) and $\lambda = 6730$ Å([S II], FWHM = 95 Å) were used. Exposure times ranged from 1800 s to 3600 s.

In all the red filters SRN has the same appearance as when observed at longer wavelengths. Figure 2 is a reproduction of the 6640 Å frame, exposure time 1 h. The northwestern lobe is bright and well defined, and the southeastern one is diffuse and fainter. The exciting star of SRN and the condensations C1 and C2 are clearly distinguished. Most of the I-stars projected against SRN are not visible; in particular, neither the double PMS star No. 10, nor the star No. 8, which is located in the dark lane close to the SRN exciting star, are detected.

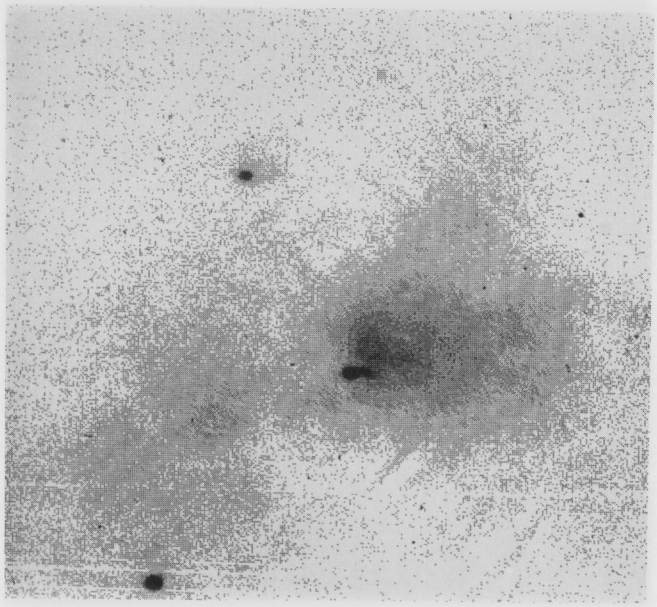

Fig. 2. CCD image of SRN at $\lambda = 6640$ Å ($\Delta\lambda = 280$ Å). Exposure time 3600 s. North is at the top and east to the left

2.3. CCD polarimetry

These observations were also made at the prime focus of the CA 3.5 m telescope in August 1985, and a near-infrared polarizer in front of the GEC CCD was used. The effective wavelength is 0.95 μm. The observations were centered at the position of SRN. Four exposures of 15 min each were made changing the position angle of the analyzer by 45° each time. The data have been reduced

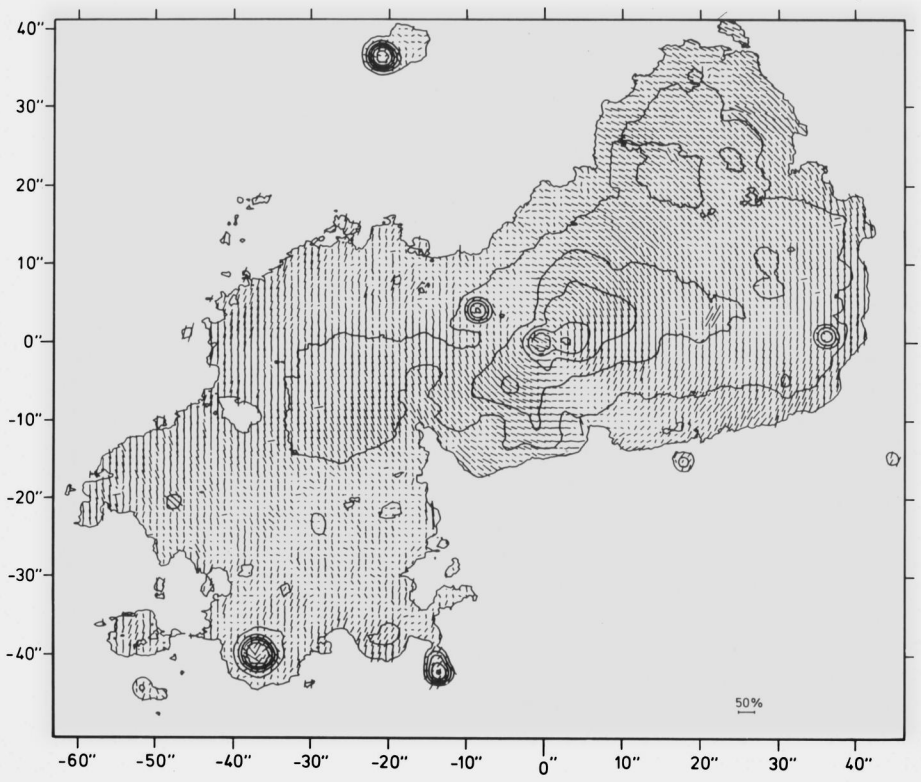

Fig. 3a. Polarization map of SRN at 0.95 µm. Electric polarization vectors are plotted with about 1″ spatial resolution. A 50% mark is given in the lower right corner. Isophotal contours are drawn with logarithmic scaling by a factor 2

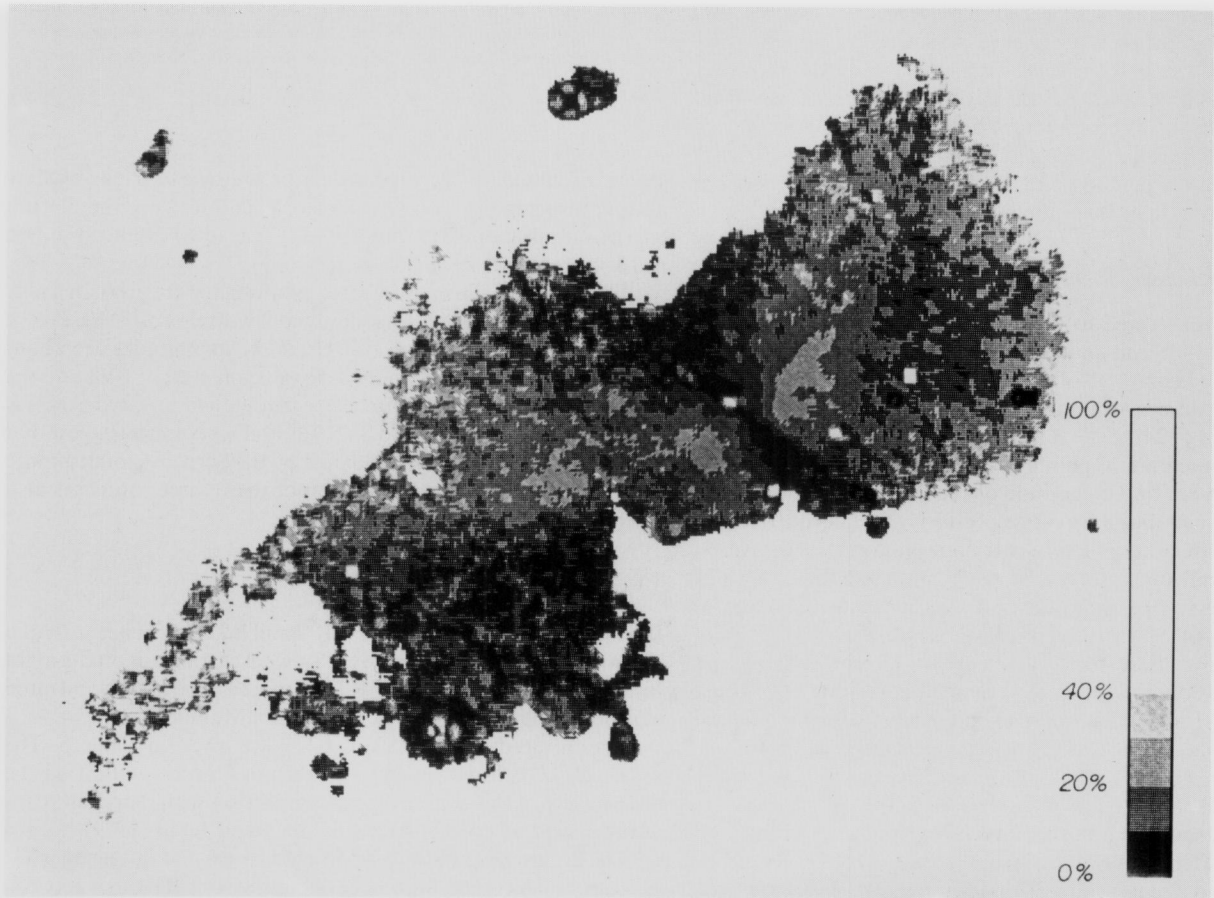

Fig. 3b. Map of polarization values in SRN at 0.95 µm. Black means polarization values below 10%, white means no significant values are found. Highest amount of polarization of 39% and 37% are found about 10″ west and 6″ southeast of the central star 6

following the procedures described by Lenzen (1987). That means that instrumental as well as constant foreground polarization is subtracted. The zero angle position is defined by laboratory measurements and has been verified on several highly polarized objects. Figure 3 shows the results of these observations. The linear polarization overlaid on an isophotal contour map is shown in Fig. 3a, and Fig. 3b is a gray scale representation of the percentage of polarization. The polarization values are plotted for S/N ratios greater than 3. Typical polarization errors are 3% in the high intensity region.

High polarization values, 30%–40%, are seen in both nebular lobes of SRN. The orientation of the electric vectors in the northwestern lobe and in the brightest parts of the southeastern lobe has a centro-symmetric pattern pointing to the central object 6. The diffuse fainter regions of the southeastern lobe have in general lower polarization values, 20% and less, and the centro-symmetric pattern breaks down. This is particulary evident in the southern regions of this lobe, where the orientation is chaotic and the percentage of polarization goes down to values smaller than 10%. A band of low polarization, less than 10%, orientated in a northeast-southwest direction along the dust lane of SRN and centered in the exciting star distorts the centro-symmetric pattern. Instead, the electric vectors are orientated almost parallel along this band and twisted close to the exciting star adopting and helicoidal pattern.

The nebular regions of SRN close to 10 present a polarization with the electric vectors orientated perpendicular to the direction of this source and, therefore, this part of the nebula is scattering light from the PMS double star. In addition, the polarimetry shows that the stars 2, 4, 8, 13, and 14 are not related to the nebulosity and so they are probably field stars. The polarimetric observations also include the cometary nebulae associated with 12 and 17. Polarization values between 10% and 20% are found in both cases, with the electric vectors orientated perpendicular to the position of the star (these data are close to our sensitivity limit). These results demonstrate that both objects are reflection nebulae scattering light from the star located at the apex.

2.4. *CA infrared observations*

These observations were carried out at the 2.2 m telescope in June 1983 and April 1985 and an InSb photovoltaic detector cooled to 55 K was used (Lenzen, 1984). Maps at 2.2 μm and 3.6 μm of a region 60″ × 90″ in size around SRN were made. A beam of 6″ and a chopper throw of 24″ to the south were chosen. The step between the different integration points was 3″ in both the α and δ directions. The limiting magnitude of the 2.2 μm and the 3.6 μm maps are 12.5 mag and 8.9 mag respectively. Standard *JHKLM* near-infrared filters were used to carry out photometric measurements of the infrared sources 10 (SVS 20), 11 (SVS 4), SVS 7, SVS 8 and SVS 9. For these observations a beam of 6″ and a chopper throw of 24″ in the δ direction were chosen.

Figure 4 shows the restored 2.2 μm map of the observed region. Five point-like sources and three extended emissions have been detected. The infrared positions of the point sources and the *K* and *L* magnitudes as deduced from the scans are given in Table 4.

All sources are also seen at 0.9 μm and, hence, the numbering in Table 4 corresponds to that in Table 2. At 2.2 μm we see a source which extends in almost opposite directions from the exciting star of SRN. This extended structure is similar to that seen at 0.9 μm at this position and represents the 2.2 μm counterpart of the brightest parts of the reflection nebula. The apparent link existing between 6 and the field star 8 is due to an effect of the beam size used. A

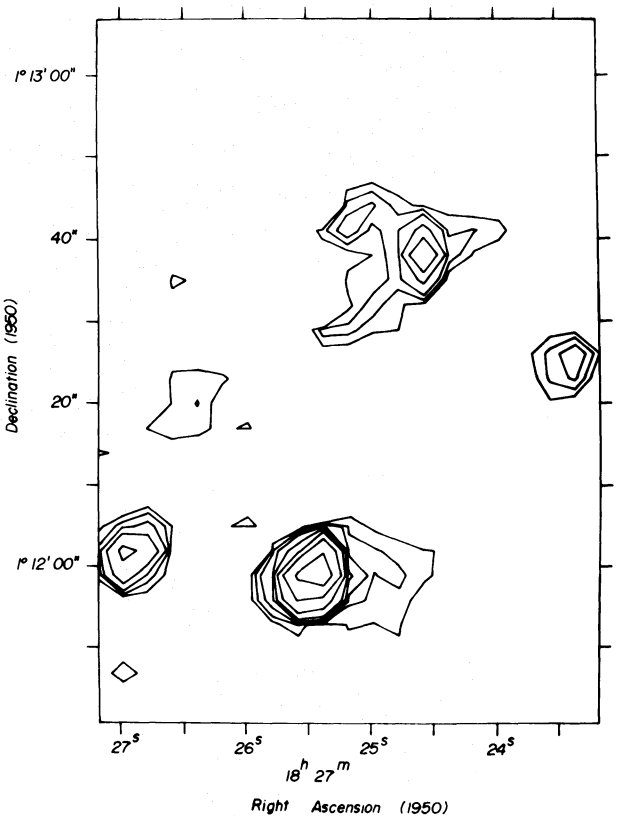

Fig. 4. 2.2 μm map of the region around SRN carried out with the CA 2.2 m telescope. The beam is 6″ and the separation of single integration points is 3″. Isocontours are drawn at levels S/N = 4, 8, 16, 32, 64, 256, and 512

second extended source is located in the southeastern lobe of SNR and approximately corresponds in position with the 0.9 μm condensations (compare with Table 3). The third extended source is associated with 10 (Eiroa et al., 1987).

The results of the near-infrared photometry are given in Table 5. The magnitudes agree reasonably well with those of SVS except in the case of 11 for which our H and K magnitudes are about 1 mag fainter. This is due to the largest beam used by SVS and the fact that 11 is a multiple source (see below). No infrared excess is detected in SVS 7, SVS 8 and SVS 9, and their colours suggest that they are background stars reddened by the Serpens cloud; a more exact determination of the position of these three sources is also given in Table 5.

2.5. *UKIRT infrared observations*

JHK photometry of the source CK 7 and a 2.2 μm raster scan of a region 20″ × 20″ in size around SVS 4 were carried out on the night June 30, 1987, using the UKIRT 3.8 m telescope and the infrared photometer UKT6 (UKIRT Observer's Manual).

The infrared magnitudes of CK 7 are given in Table 5. The $J-H$, $H-K$ colours show a clear infrared excess indicating the PMS nature of this source. For a comparison with representatives of these kind of objects see e.g. Cohen and Kuhi (1979).

The 2.2 μm map of the SVS 4 field was carried out using a 3.″1 aperture and a chopper throw of 20″ to the west. The step between the different integration points was 2″ in both α and δ directions. The results are shown in Fig. 5 and reveal that there are at least 5

Table 4. Positions and K and L magnitudes of Serpens point sources from the infrared scans at the CA 2.2 m telescope. Position error is 3″

Object	α(1950)	δ(1950)	K	L
4	$18^h27^m23^s.4$	1°12′26″.0	10.8 ±0.2	>8.9
6	$24^s.6$	12′41″.0	8.93±0.04	7.1 ±0.4
8	$25^s.2$	12′44″.0	11.6 ±0.3	>8.9
10	$25^s.4$	11′59″.0	7.00±0.02	4.92±0.08
13	$27^s.0$	12′02″.0	9.42±0.07	7.8 ±0.4

Table 5. Positions and near infrared photometry of some Serpens objects. Position error is 3″

Object	α(1950)	δ(1950)	J	H	K	L	M
10 (SVS20)	$18^h27^m25^s.38$	1°11′58″.6	11.97±0.20	9.04±0.10	6.97±0.01	4.93±0.01	4.3±0.1
11 (SVS4)	$25^s.44$	10′42″.9		12.30±0.10	9.85±0.07	8.24±0.09	7.3±0.3
SVS7	$36^s.6$	12′32″.0	12.29±0.09	9.87±0.04	8.92±0.30	8.84±0.06	>7.3
SVS8	$39^s.8$	13′23″.0	12.26±0.20	9.67±0.01	8.78±0.01	8.39±0.01	>7.3
SVS9	$12^s.7$	16′35″.0	12.50±0.17	9.99±0.01	8.57±0.01	8.17±0.04	7.2±0.2
CK7	$29^s.3$	11′54″.0	16.29±0.06	14.42±0.02	12.74±0.01		

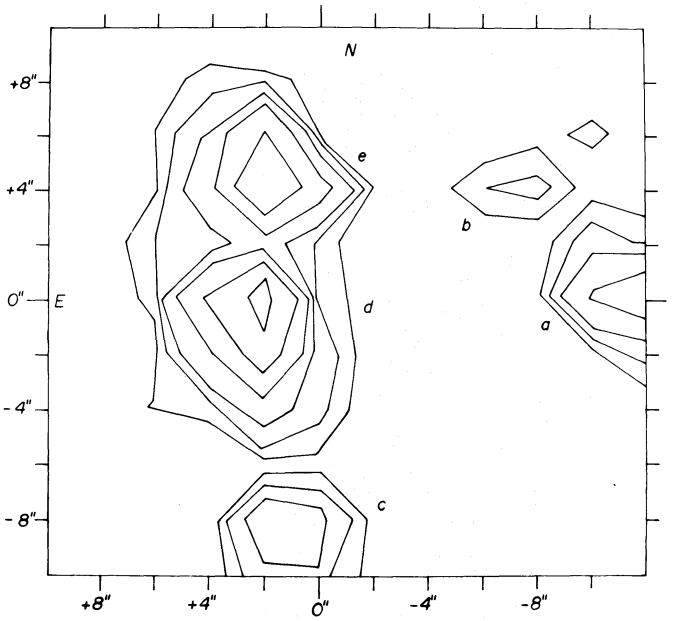

Fig. 5. 2.2 μm map of SVS 4 carried out with the UKIRT 3.8 m telescope. The beam used is 3″ and the separation of single integration points 2″. Isocontours are drawn at levels S/N = 3, 6, 12, 24, 48, and 96. Position (0, 0) corresponds to the position of the object 11 in Table 2. North is at the top and east to the left

individual point-like sources within the region known as the infrared source SVS 4 (in fact, the beam used by SVS was larger than our mapped field). The position and estimated K magnitude of each SVS 4 object is given in Table 6. One source, SVS 4d, coincides within the positional error with the radio source found by Rodriguez et al. (1980) and with our object 11, the faint bipolar nebula. A second source, SVS 4e, is located 4″ to the north. The K magnitude of SVS 4 given in Table 5 results from the contribution of these two sources to the flux within the 6″ beam used in the Calar Alto observations. Our data are insufficient to decide if the other three sources are members of the Serpens cloud or if they are background stars.

Table 6. Positions and K magnitudes of the sources in the SVS4 field as estimated from the UKIRT scans. Position error is 2″

Source	α(1950)	δ(1950)	K
SVS4a	$18^h27^m24^s.6$	1°10′43″.0	11.43±0.04
SVS4b	$24^s.9$	47″.0	13.11±0.08
SVS4c	$25^s.6$	33″.0	12.24±0.08
SVS4d	$25^s.6$	43″.0	10.25±0.02
SVS4e	$25^s.6$	47″.0	10.58±0.02

3. Discussion

3.1. *The nature of the Serpens nebulosities: extinction*

Seven nebulosities are seen in our CCD images: two bipolar and five cometary nebulae. As noted before the polarization data show that SRN is a reflection nebula illuminated by the stellar object 6, as previously found by Worden and Grasdalen (1974). The nebulosities associated with the stars 12 ad 17 have the same reflection nature. Infrared polarimetry at 2.2 μm of 17 using a beam of 12″ in size carried out at our request by K.W. Hodapp on Calar Alto Observatory yields $p = 4.3\% \pm 0.3\%$ at a polarization angle of 41° ± 1°. This is a further confirmation of the scattering origin of this nebula. HL showed that 18 (GGD 29) is not an HH object. In addition, we know that there are no high luminosity sources in the Serpens cloud (Nordh et al., 1982; Harvey et al., 1984). Assessing these results together with the similar appearance in the 0.9 μm images, we believe that all Serpens nebulosities are reflection nebulae.

Chavarria et al. (1987) recently estimated the interstellar reddening to the Serpens region. Their value, $A_v = 2.7$ mag, is a

Table 7. ΔA_v from Hubble's relation and position angle of the major axis of the Serpens nebulae and of FIRS 1

Object	ΔA_v (mag)	Position angle
5	5.0	147°
11		25°
12	0.2	124°
15	4.8	131°
17	3.7	144°
18	0.2	140°
SBN	7.3	123° [a]
SBN		125° [b]
FIRS 1		130° [c]
Mean angle [d]		133°

[a] From isocontours
[b] Perpendicular to the polarization band
[c] From Fig. 13 of Snell and Bally (1986)
[d] Excluding object 11

lower limit of the extinction suffered by the Serpens objects. In the case of the stars exciting the reflection nebulae, this lower limit can be improved by means of the Hubble's relation which provides an estimate of the differential extinction between the stars and the nebulosities (Castelaz et al., 1985; Lenzen, 1987). The method relates the radial extension of the nebula with the limiting surface brightness and the observed magnitude of the star. Table 7 gives the ΔA_v values (extinction to the star minus extinction to the nebula) for all seven Serpens nebulous objects. The angular size has been taken as given by the 3σ isocontour level except in the cases of 12 and 15, where the 6σ level has been considered in order to avoid confusions produced by the SRN extended emission, see Fig. 6. The northwestern lobe of SRN has been considered, as it seems to be free from the distorting effects seen in the other lobe (e.g. illumination by 10). We have also assumed that the ratio A_I/A_v is given by a normal extinction law (Rieke and Lebofsky, 1985) although Chavarria et al. (1987) found the ratio $R = A_v/E(B-V) = 4$, departing from the normal value of 3. The main conclusion deduced from the ΔA_v values is that in all the cases the extinction to the star is larger than the extinction to the associated nebulosity. Only for 12 and 18 the extinction to the stars and to the nebulae are of the same order. It is worth mentioning that our assumed reddening law does not affect this qualitative result. The simplest explanation is that dust located in the line of sight to the stars produces the additional extinction. In the cases of SRN and 11 the classical model of bipolar nebulae account for this fact (Elsässer and Staude, 1978). We now know

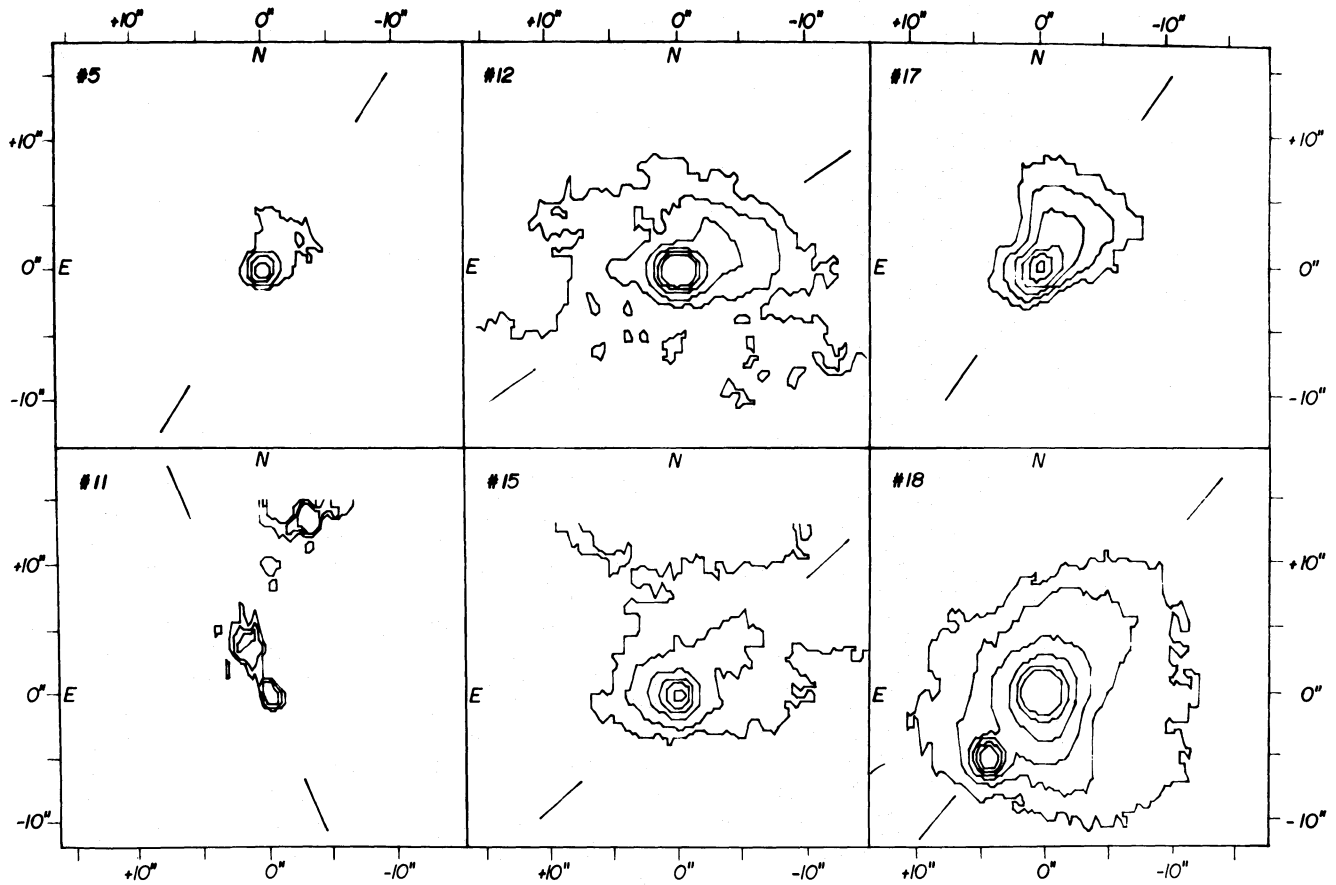

Fig. 6. Isocontours maps of the Serpens nebulosities. In all cases the point (0,0) refers to the position given in Table 2. Isocontours are drawn at levels S/N = 3, 6, 12,... The short straight lines plotted in each square of the figure indicate an estimate of the major axis of the nebulosities

that many of the cometaries, and perhaps all, are bipolar, the second lobe being directed into the ambient molecular cloud and/or obscured by an equatorial, optically thick dust disk which prevents the direct observation of the lobe. R Mon/NGC 2261 and PV Cephei are two bona-fide optically cometary nebulae, which are indeed bipolar (Warren-Smith et al., 1987b; Neckel et al., 1987). Such a phenomenon could be occurring in several or all Serpens cometary nebulae; in this case, the second SE lobe would be buried in the molecular cloud and/or hidden by circumstellar dust disks or tori. In fact, we observe this effect in SRN, which is tilted to our line of sight. The northwestern lobe is bright, easily detected in all wavelengths, as expected if it is directed out of the molecular cloud toward the observer; the southeastern lobe is more obscured and embedded in the cloud. Other direct sign of the tilt of SRN is based on the fact that some parts of this latter lobe are illuminated by the star 10, which is deeper embedded in the cloud than the SRN exciting star, as the 3.1 μm ice optical depth shows (CK, Eiroa and Hodapp, in preparation). The cases of 12 and 18, where we do not see a clear reddening of the stars with respect to the nebulosities, could be explained if we see both objects projected near pole-on.

3.2. *The alignment in Serpens and the role of the magnetic field*

Bipolar and cometary nebulae are admitted to be optical manifestations of outflows resulting from mass-loss processes in young stellar objects (e.g. Kaifu, 1987).

A characteristic common of the Serpens optical outflows is the alignment of their projected symmetry axis. Table 7 gives the position angle of this axis for each object; the angle is measured from north to east (Fig. 6). For SRN we have considered the northwestern lobe; the perpendicular to the noncentro-symmetric polarization band is also given. Only the bipolar nebula 11 departs from the common orientation. Snell and Bally (1986) have detected three compact sources associated with FIRS 1. The sources are aligned in a direction similar to that defined by the axis of the Serpens nebulae, Table 7. Although the observations do not provide a definitive picture of the radio sources, a stellar wind nature is favoured by the far-infrared and radio data, and now indirectly by the common alignment of the radio sources with the optical outflows. Therefore, at least eight objects in the Serpens cloud are undergoing a phase of noticiable mass-loss.

Optical polarization measurements of the field stars show that the magnetic field has a component perpendicular to the galactic plane in this region (Mathewson and Ford, 1970), which is due to the effect of the helical component of the local magnetic field (Mathewson, 1968). In Fig. 7 we have plotted in equatorial coordinates the orientation of the mean Serpens outflow axis (excluding 11), the galactic plane, and the helical component of the magnetic field as inferred from a visual inspection of Figs. 1 and 5a of Mathewson (1968) and Mathewson and Ford (1970). The figure clearly illustrates the alignment between the mean outflow axis of the Serpens objects and the magnetic field. Similar alignments have been found in different outflow sources (Cohen et al., 1984; Hodapp, 1984; Sato et al., 1985; Strom et al., 1986). These results strongly suggest that the mass-loss processes in Serpens occur along the magnetic field lines permeating the cloud; these lines are probably linked with those threading the entire region. They also suggest that the initial collapse, which eventually led to the formation of the Serpens objects, took place along the interstellar field lines.

It is well known that contracting molecular clouds tend to form flattened structures (Mestel, 1977; Mestel and Paris, 1984).

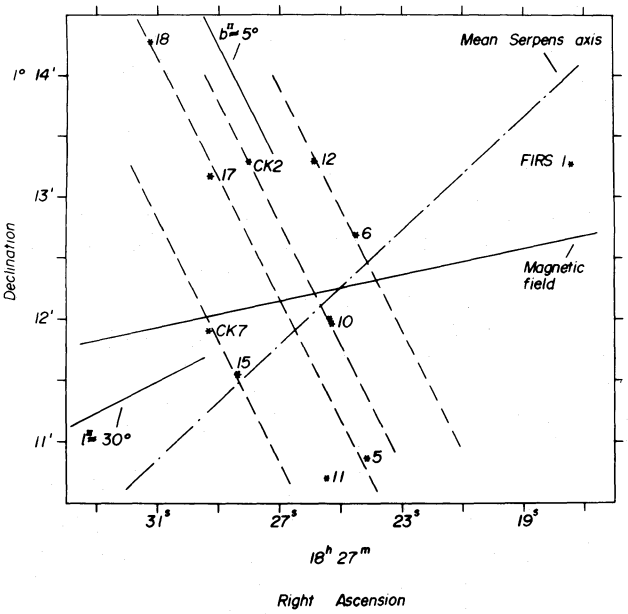

Fig. 7. Plot in equatorial coordinates showing the orientation of the helical component of the local magnetic field (———) the mean position angle of the Serpens outflow objects (–·–) and lines of b^{II} = const (– – –). The position of all known young Serpens objects is also plotted

Under the influence of rotation and magnetic field, pancakes or disks with protostellar cores are formed. As a result, aligned outflows would show up. This scenario has recently been studied by Pudritz and Silk (1987), and could be a suitable sketch for Serpens. The collapse of the magnetic cloud would also lead to the formation of a sheet-like configuration with the individual dense layers orientated perpendicular to the magnetic field, and separated by a distance comparable to the Jeans length (Moneti et al., 1984; Pudritz and Silk, 1987). The Taurus cloud shows such a stratified structure, which has been attributed to the effect of the magnetic field during the early stages of collapse (Moneti et al., 1984; Tamura et al., 1987). In the case of Serpens, the outflow sources seem to be located along the lines of b^{II} = const. Objects 6 and 12 form a group with the same galactic latitude, whereas 5, 17, and 18 form a second group (Fig. 7). Moreover, the objects 15 and CK 7 and 10 and CK 2 would form a third and fourth group respectively. One could speculate that the Serpens PMS objects are located in layers stratified and perpendicular to the magnetic field. The layers have a projected separation in the range of 18″ to 36″, which corresponds to 0.02 to 0.04 pc. The Jeans length in Serpens is $L_J = 0.11$ pc, taking as temperature and mass of the Serpens core 20 K and 220 $M_\odot$ (Loren et al., 1979). This value is higher than the observed sheet separation in Serpens, although we do not think that this discrepancy is sufficient to rule out our speculation. In fact, the arrangement of young objects along lines parallel to the galactic plane, hence perpendicular to the magnetic field, has a remarkable statistical weight. From the 11 young objects within the field covered by our observations, 9 are projected along lines parallel to the galactic plane (Fig. 7); on the other hand, the observational data are insufficient to clarify whether there exist, or not, more young objects along the b^{II} direction of FIRS 1.

Finally, the formation of binary systems in a flattened magnetic cloud would take place in cloud structures probably similar to the pancakes of Pudritz and Silk (1987), and orientated

perpendicularly to the magnetic field. In this sense it is noteworthy that the projected alignment of the PMS double source 10 lies in a plane nearly perpendicular to the magnetic field. Fig. 7 (Eiroa et al., 1987).

3.3. *Star formation efficiency and stellar density*

The conversion of gaseous mass into stars and the density of young stars in molecular clouds are important figures for the theory of molecular clouds and the formation of stellar associations and open clusters (Wilking and Lada, 1985). The fraction of gas converted into stars is usually computed by means of the parameter η, the star formation efficiency, defined as $\eta = M_{\rm stars}/(M_{\rm stars} + M_{\rm gas})$. A reliable estimate of η and of the stellar density is difficult to give mainly because of the uncertainties affecting the number of stars associated with the cloud, their masses and the mass of the molecular cloud itself. In spite of this, a rough estimate of both parameters is very useful because it contains helpful information about the aforementioned figures.

The 0.9 μm images together with the infrared results provide a reasonable estimate of the number and mass of young stellar objects formed in the dense 220 $M_\odot$ Serpens core (Loren et al., 1979). All the 7 stellar objects associated with nebulosity lie inside this core; the infrared colours also confirm the PMS nature of three of these objects (SVS, CK, this work). Three other PMS objects are 10, CK 2 and CK 7. Finally, the far infrared source FIRS 1 also lies within the core. This means, that at least 12 young objects (10 is double) are clustered in the Serpens dense core. Here, we have considered that only the source SVS 4d belongs to the Serpens cloud; but see below for a further discussion. Protostellar objects of 1–2 $M_\odot$ explain the observed infrared properties of CK 2 and of each component of 10 (Wolfire and Churchwell, 1987; Eiroa and Leinert, 1987). From far-infrared observations we know that there are no massive, very luminous objects in Serpens (Nordh et al., 1982; Harvey et al., 1984). These results indicate that there is at least a cluster of 12 objects of masses in the range 1–2 $M_\odot$ inside the 0.24 pc radius of the Serpens core. A star formation efficiency of 6% and a stellar density of 240 $M_\odot$ pc^{-3} are implied, assuming a mass of 3 $M_\odot$ for the double 10, 2 $M_\odot$ for CK 2 and 1 $M_\odot$ for the rest of the cluster members. Both values have to be regarded as lower limits, as the following considerations demonstrate.

First, the field recovered by the *I* images represents 60% of the surface of the core. If we assume that in the unobserved core region the same proportion of young objects exists, values of 8.3% and 340 $M_\odot$ pc^{-3} could be expected. Second, some of the SVS4 objects, of the *I* stars, and of the *K* sources of CK, for which a classification is not possible yet because of the scarce available data, could also be members of the young Serpens cluster. Third, we might have failed to detect objects of very low mass, hence of very low luminosity, because of the selection effects introduced by the sensitivity limits; in other words, the sample can be biased because the optical depth to which stars are sampled, varies with the luminosity. Summarizing, it seems reasonable to expect a star formation efficiency of around 10% and stellar densities of several hundreds $M_\odot$ pc^{-3}.

In the last few years values of η have been calculated for other dark molecular clouds and cores (Vrba, 1977; Wilking and Lada, 1985 and references therein). Except in very few cases, the results indicate that the efficiency to convert gas into stars is rather modest. In this sense, the η value of Serpens is normal. The stellar density, however, departs from typical values found in these clouds and even the uncorrected value exceeds that of the ϱ Ophiuchi infrared cluster (Lada and Wilking, 1984). The high density is produced by the degree of concentration of low mass PMS stars in the Serpens core and strongly suggests that the young Serpens cluster will be converted into a gravitacionally bounded cluster after the gas cloud is removed.

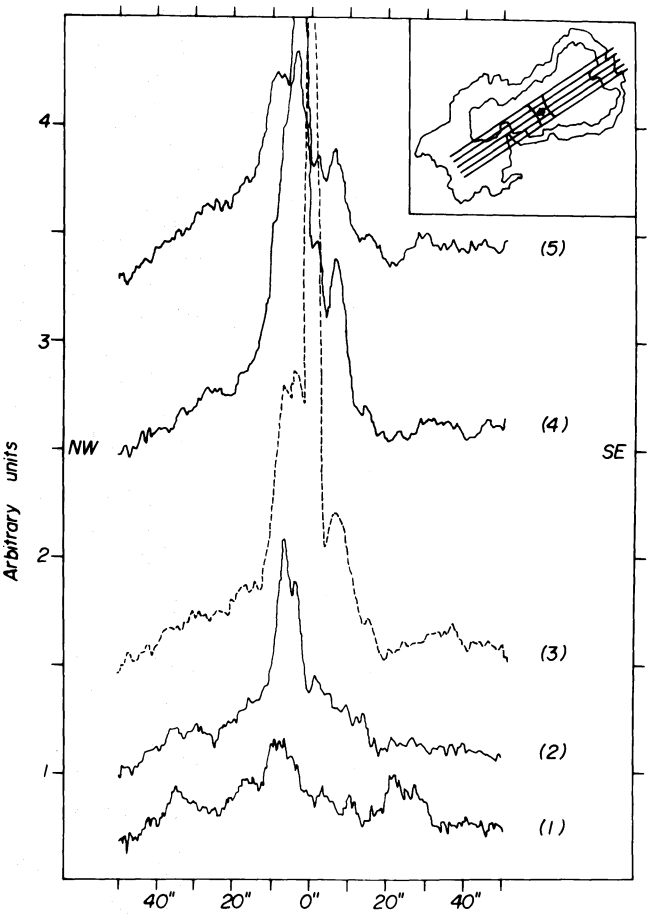

Fig. 8. Intensity profiles in the band I along five lines perpendicular to the polarization band of SRN, as indicated in the sketch shown in the upper-right part of the figure. (1) is the line located most toward the north, whereas (3) runs through the maximum of the illuminating star 6 and (5) is the line located to the south. Position 0″ is the intersection of each line with the plane of the polarization band running through 6. A narrow dark lane very close to 6 can be observed from the intensity profiles, and its outer edges are shown in the sketch

3.4. *The Serpens reflection nebula (SRN)*

Two distinct patterns are drawn by the polarization vectors in SRN: the centro-symmetric orientation of the electric vectors in the nebular lobes, and the band of low polarization around 6 and perpendicular to the major axis of SRN. Similar results have been found by King et al. (1983) and Warren-Smith et al. (1987a).

An almost identical behaviour of the polarization has been observed in other reflection nebulae, e.g. Ward-Thompson et al. (1985), as well as in several evolved bipolar nebulae (Schmidt et al., 1978; Taylor and Scarrot, 1980). Figure 8 shows the intensity profiles in the *I* band along five lines perpendicular to the polarization band. A narrow dark lane, angular size from ~5″ to 8″, parallel to the polarization band is found. A similar obscuration is seen in the $\lambda = 6640$ Å image and has also been noticed by Warren-Smith et al. (1987a). These facts indicate the existence of a dust

band probably in the form of a disk or torus around the central star 6.

An interpretation of these results has to take into account the following features: 1. The alignment of the major axis of SRN with the magnetic field, 2. The centro-symmetric pattern of the polarization in the nebular lobes. 3. The dust disk or torus with the noncentro-symmetric band oriented perpendicular to the magnetic field.

The polarization in the lobes can be explained by the scattering mechanism in bipolar nebulae (Elsässer and Staude, 1978). This mechanism cannot, however, account for the observed polarization in the dust disk.

A model explaining the noncentro-symmetric polarization band has been proposed by Notni (1985). Notni's model explains the polarization band by single scattering in a dusty medium. Depending on the polarization of the central source and on the optical depth of the medium, the pattern can be elliptical or parallel to the polarization of the central star. No alignment of the scattering grains needs to be assumed; the role of the magnetic field is meaningless. In this model the disk of SRN would be a medium of nonaligned dust particles detached from the Serpens magnetic field.

A second alternative is that the polarization band arises from extinction by aligned grains. In that case the alignment mechanism would be a toroidal magnetic field frozen-in with the dust disk, and perpendicular to the field permeating the Serpens cloud. The orthogonality of both fields could be explained in terms of a magnetized cloud; namely, a part of an interstellar cloud with a large scale interstellar magnetic field condenses due to gravitational collapse. The condensing mass converts into a central protostellar object and a rotating disk; the field lines are twisted and wound by the rotation of the disk (Uchida and Shibada, 1985; see also Pudritz and Norman, 1986). Such a framework seems to be reasonably suitable for all the observed features in Serpens since the role of the magnetic field appears to be notorious, as demonstrated by the orientation of the nebulae, of the FIRS 1 radio sources, and of the double No. 10. Therefore, we suggest this is the physical mechanism originating the noncentro-symmetric polarization band.

We now have to point out that our explanation of the SRN polarization differs from the picture of King et al. (1983) and Warren-Smith et al. (1987a). They suggest that the polarization band reflects the direction of the galactic field. We believe, however, this is erroneous for the observed alignment of the Serpens objects strongly claims that the galactic field is perpendicular to the polarization band.

The dust disk produces an extinction of around 7 mag, Table 7. This value has to be added to the approximately 3 mag of interstellar reddening to the Serpens region (Chavarria et al., 1987) in order to estimate the total extinction to the exciting star 6. Our results back previous estimates of the extinction of 8 mag (King et al., 1983), rather than the lower value given by Cohen and Kuhi (1979). The comparison of the near-infrared observations probably indicates that 6 is variable, although we have to be cautious because of the contamination produced in the different beams by the nebulosity close to the star (SVS, CK, Harvey et al., 1984; this work). In any case the infrared colours show an infrared excess, which is probably due to a dust envelope around the star, independent of the large-scale dust disk. The bolometric luminosity lies in the range between 0.6 and 20 $L_{\odot}$. The lower limit is estimated from the uncorrected $I-K$ colour temperature whereas the upper limit results from far-infrared measurements. In short, the exciting star of SRN seems to be a young low mass star surrounded by a dust envelope.

3.5. The new bipolar nebula associated with No. 11

A tiny very faint nebulosity appears at the position of the southern radio source of the field (Rodriguez et al., 1980). The size of the nebulosity is $\sim 6''$, corresponding to 0.0073 pc and it has a bipolar morphology with a central dark band of approximately 4.8 10^{15} cm wide. A point-like source is located at the south-eastern lobe close to the central dark band, and it probably marks the position of the exciting star. This is object 11 in Table 2. This is also the position of the near infrared source SVS 4d. The close source SVS 4e can be a field star, a Serpens star, or a kind of infrared nebulosity. If SVS 4e is another member of the Serpens young cluster, it would probably form together with 11 (SVS 4d) the second double star known within the Serpens cloud core; in this case the projected separation of the double is 1000 AU. If SVS 4e is an infrared nebulosity, it does not coincide with the northeastern lobe of the 0.9 μm nebula, since the relative orientation of SVS 4d and SVS 4e is clearly different to that of the bipolar nebula.

The position angle of the bipolar axis is 25°. Thus, the nebula is orientated almost parallel to the galactic plane, and perpendicular to the other Serpens nebulosities. This singular behaviour questions the membership of 11 to the Serpens PMS cluster. The velocity of the molecular emission at this position is similar to that of other points of the cloud, and the kinetic temperature reaches a value of 27 K (Loren et al., 1979). The far infrared radiation of the Serpens cloud extends toward 11 (Nordh et al., 1982). CO high velocity wings have been detected near the source (Nordh et al., 1982). The bolometric luminosity deduced from far-infrared observations is 22.5 $L_{\odot}$, and is much smaller than the luminosity deduced from radio continuum measurements (Harvey et al., 1984; Snell and Bally, 1986). All these facts suggests, but do not demonstrate, that 11 does belong to the Serpens cloud.

Several other outflow sources are known to be misaligned with the local magnetic field; examples are GL 490 (Cohen et al., 1984), L 1689N (Wooten and Loren, 1987), and the outflow associated with HH 12 (Heyer et al., 1987). In addition, the statistics of Strom et al. (1986) suggest that 30% of the outflows are not aligned to within 30° of the field direction. The physical circumstances producing the misalignment are still unclear; Wooten and Loren (1987) suggest that the deflection of the L 1689N flow by a cold clump could be the origin of the misalignment, meanwhile Heyer et al. (1987) speculate that it could be a result of insufficient ionization of the cloud core associated with the corresponding young stellar object.

4. Conclusions

1. At least 11 PMS stars (one is double) are clustered in the core of the Serpens molecular cloud. They will form a gravitationally bounded cluster after the gas of the cloud is removed.

2. We found that eight objects are in a evolutionary stage of asymmetric mass loss. The mass loss occurs along the lines of the interstellar magnetic field as suggested by the alignment of the major axis of the Serpens outflows and the magnetic field. The plane of the PMS double star is also related to the direction of the magnetic field.

3. The PMS Serpens objects seem to be located within a sheet-like structure orientated perpendicular to the magnetic field.

4. The polarization of SRN can be explained in terms of light scattered by dust grains within the nebular lobes and extinction by a disk of aligned dust grains. The alignment mechanism is the magnetic field, frozen-in with the disk; this has its ultimate origin

in the initial collapse of a magnetized fragment of the Serpens cloud and the twist of the magnetic field lines. The heliocoidal shape of the polarization band around the exciting star is due to the superposition of both polarization patterns.

5. A tiny bipolar nebulosity has been found at the position of the southern Serpens radio source. This object is peculiar as indicated by the misalignment of the nebula with respect to any other Serpens object. Two infrared sources found in this position, SVS 4d and SVS 4e, could form the second double star known in the Serpens core.

Acknowledgements. A.I.G. de C. is supported by a fellowship of the Comunidad Autonoma de Madrid. The stay of C.E. at the University of Hawaii's Institute for Astronomy was granted by the US-Spanish Joint Committee for Scientific and Technological Cooperation, and he is grateful to Dr. D.N.B. Hall for his hospitality at IfA. We thank the staffs of the Calar Alto observatory and UKIRT for their assistance during the observations, as well as ESA for the use of their computer facilities in VILSPA.

References

Bally, J., Lada, C.J.: 1983, *Astrophys. J.* **265**, 824
Blair, G.N., Davis, J.H., Dickinson, D.F.: 1978, *Astrophys. J.* **226**, 435
Castelaz, M.W., Hackwell, J.A., Grasdalen, G.L., Gehrz, R.D., Gullixson, C.: 1985, *Astrophys. J.* **290**, 261
Chavarria, K.C., Ocegueda, J., de Lara, E., Finkenzeller, U., Mendoza, E.: 1987, *IAU Symp.* **122**, Reidel, Dordrecht, p. 97
Churchwell, E., Koornneef, J.: 1986, *Astrophys. J.* **300**, 729
Clark, F.O., Turner, B.E.: 1987, *Astron. Astrophys.* **176**, 114
Cohen, M., Kuhi, L.V.: 1979, *Astrophys. J. Suppl.* **41**, 743
Cohen, R.J., Rowland, P.R., Blair, M.M.: 1984, **210**, 425
Dinger, A.St.C., Dickinson, D.F.: 1980, *Astron. J.* **85**, 1247
Eiroa, C., Leinert, Ch.: 1987; *Astron. Astrophys.* **188**, 46
Eiroa, C., Lenzen, R., Leinert, Ch., Hodapp, K.W.: 1987, *Astron. Astrophys.* **179**, 171
Elsässer, H., Staude, H.J.: 1978, *Astron. Astrophys.* **70**, L3
Gyulbudaghian, A.L., Glushkov, Yu.I., Denisyuk, E.K.: 1978, *Astrophys. J. Letters* **224**, L137
Hartigan, P., Lada, C.J.: 1985, *Astrophys. J. Suppl.* **59**, 383
Harvey, P.M., Wilking, B.A., Joy, M.: 1984, *Astrophys. J.* **278**, 156
Heyer, M.H., Strom, S.E., Strom, K.M.: 1987, *Astron. J.* **94**, 1653
Ho, P.T.P., Barrett, A.H.: 1980, *Astrophys. J.* **237**, 38
Hodapp, K.-W.: 1984, *Astron. Astrophys.* **141**, 255
Kaifu, M.: 1987, in *Star Forming Regions, IAU Symp.* **115**, (Reidel, Dordrecht), p. 275
King, D.J., Scarrott, S.M., Taylor, K.N.R.: 1983, *Monthly Notices Roy. Astron. Soc.* **202**, 1087
Lada, C.J., Wilking, B.A.: 1984, *Astrophys. J.* **287**, 610
Lenzen, R.: 1984, Calar Alto Observatory Infrared Photometer Manual
Lenzen, R.: 1987, *Astron. Astrophys.* **173**, 124
Little, L.J., Brown, A.T., McDonalds, G.H., Riley, P.W., Matheson, D.N.: 1980, *Monthly Notices Roy. Astron. Soc.* **193**, 115
Loren, R.B., Evans, II, N.J., Knapp, G.R.: 1979, *Astrophys. J.* **234**, 932
Loren, R.B., Plambeck, R.L., Davis, J.H., Snell, R.L.: 1981, *Astrophys. J.* **245**, 495
Loren, R.B., Wootten, A.: 1980, *Astrophys. J.* **242**, 568
Mathewson, D.S.: 1968, *Astrophys. J. Letters* **153**, L43
Mathewson, D.S., Ford, V.L.: 1970; *Mem. Roy. Astron. Soc.* **74**, 139
Mestel, L.: 1977, in *Star Formation, IAU Symp.* **75**, eds. T. de Jong, A. Maeder, (Reidel, Dordrecht), p. 213
Mestel, L., Paris, R.B.: 1984, *Astron. Astrophys.* **136**, 98
Mirabel, I.F.: 1987, in *Star Forming Regions, IAU Symp.* **115**, (Reidel, Dordrecht), p. 315
Moneti, A., Pipher, J.L., Helfer, H.L., McMillan, R.S., Perry, M.L.: 1984, *Astrophys. J.* **282**, 508
Neckel, T., Staude, H.J., Sarcander, M., Birkle, K.: 1987, *Astron. Astrophys.* **175**, 231
Nordh, H.L., Van Duinen, R.J., Sargent, A.I., Fridlund, C.V.M., Aalders, J.W.G., Beintema, D.: 1982, *Astron. Astrophys.* **115**, 308
Notni, P.: 1985, *Astron. Nachr.* **306**, 265
Pudritz, R.D., Norman, C.E.: 1986, *Astrophys. J.* **301**, 571
Pudritz, R.D., Silk, J.: 1987, *Astrophys. J.* **316**, 213
Rieke, G.H., Lebofsky, M.J.: 1985, *Astrophys. J.* **288**, 618
Rodriguez, L.F., Moran, J.M., Dickinson, D.F., Gyulbudaghian, A.L., 1978, *Astrophys. J.* **226**, 115
Rodriguez, L.F., Moran, J.M., Ho, P.T.P., Gottlieb, E.W.: 1980, *Astrophys. J.* **235**, 845
Sato, S., Nagata, T., Nakajima, T., Nishida, M., Tanaka, M., Yamashita, T.: 1985, *Astrophys. J.* **291**, 708
Schmidt, G.D., Angel, J.R.P., Beaver, E.A.: 1978, *Astrophys. J.* **219**, 477
Sharpless, S.: 1959, *Astrophys. J. Suppl.* **4**, 257
Snell, R.L., Bally, J.: 1986, *Astrophys. J.* **303**, 683
Strom, S.E., Grasdalen, G.L., Strom, K.M.: 1974, *Astrophys. J.* **191**, 111
Strom, K.M., Strom, S.E., Wolff, S.C., Morgan, J., Wenz, M.: 1986, *Astrophys. J. Suppl.* **62**, 39
Strom, S.E., Vrba, F.J., Strom, K.M.: 1976, *Astron. J.* **81**, 638
Tamura, M., Nagata, T., Sato, S., Tanaka, M.: 1987, *Monthly Notices Roy. Astron. Soc.* **224**, 413
Taylor, K.N.R., Scarrott, S.M.: 1980, *Monthly Notices Roy. Astron. Soc.* **193**, 321
Uchida, Y., Shibata, K.: 1985, *Publ. Astron. Soc. Japan* **37**, 515
Ungerechts, H., Gusten, R.: 1984, *Astron. Astrophys.* **131**, 177
Vrba, F.J.: 1977, *Astron. J.* **82**, 198
Ward-Thompson, D., Warren-Smith, R.F., Scarrott, S.M., Wolstencroft, R.D.: 1985, *Monthly Notices Roy. Astron. Soc.* **215**, 537
Warren-Smith, R.F., Draper, P.W., Scarrot, S.M.: 1987a, *Monthly Notices Roy. Astron. Soc.* **227**, 749
Warren-Smith, R.F., Draper, P.W., Scarrott, S.M.: 1987b, *Astrophys. J.* **315**, 500
Wilking, B.A., Lada, C.J.: 1985; *Protostars and Planets II*, eds. D.C. Black, M.S. Matthews, University of Arizona Press, Tucson, p. 297
Wolfire, M.G., Churchwell, E.: 1987, *Astrophys. J.* **315**, 315
Wooten, A., Loren, R.B.: 1987, *Astrophys. J.* **317**, 220
Worden, S.P., Grasdalen, G.L.: 1974, *Astron. Astrophys.* **34**, 37